ChemComm

COMMUNICATION

View Article Online
View Journal | View Issue

Cite this: *Chem. Commun.*, 2024, **60**, 2625

Received 17th January 2024,
Accepted 31st January 2024

DOI: 10.1039/d4cc00254g

rsc.li/chemcomm

Arbuzov meets 1,2-oxaphosphetanes: transient 1,2-oxaphosphetan-2-iums as an entry point to beta-halo phosphane oxides and P-containing oligomers†‡

Florian Gleim,[a] Gregor Schnakenburg,[a] Arturo Espinosa Ferao *[b] and Rainer Streubel *[a]

Herein, we describe the synthesis of a 1,2$\sigma^3\lambda^3$-oxaphosphetane from ethylene oxide and its reactions with alkyl halides to form β-halo phosphane oxides in an Arbuzov-type reaction. When methyl triflate was used as a hard electrophile, cationic oligomerisation of 1,2-oxaphosphetanes was observed. DFT calculations indicate 1,2-oxaphosphetan-2-iums as intermediates and reveal differences between the Arbuzov and the potential Perkow reaction pathway.

Strained organic and inorganic ring systems[1] are highly interesting due to their special bonding situation and high reactivity. For example, oxetanes (**I**) (Fig. 1) are important building blocks for synthesising more complicated molecules[2] and polymers.[3] The phosphorus-containing four-membered rings such as phosphetanes (**II**) drew attention because of their use as steering ligands in transition metal catalysis,[4] and, more recently, as organocatalysts.[5–10] Oxaphosphetanes (**III**, **IV**) represent an unusual combination of oxetanes and phosphetanes but have been scarcely studied, so far. It can be anticipated that 1,3-oxaphosphetanes (**III**)[11] and 1,2-oxaphosphetanes (**IV**)[12] will behave quite differently whereby **III** should possess features more similar to **I** and **II**. Interestingly, higher coordinate derivatives of **III** and **IV** have been investigated more often. For example, 1,3$\sigma^4\lambda^5$-oxaphosphetanes are available through intramolecular Mitsunobu reactions,[11] and bi- and tricyclic 1,3$\sigma^3\lambda^3$-oxaphosphetanes have recently been proposed in the decomposition of HPCO.[13] The 1,2$\sigma^5\lambda^5$-oxaphosphetanes (**IVb**) were discussed as intermediates in the lithium-free Wittig reaction,[12,14,15] and also in the deoxygenation of epoxides.[15–17] Recent DFT calculations showed that they also occur in the phosphite-initiated reductive dimerization of ketones.[18] Until now, very few crystal structures of 1,2$\sigma^5\lambda^5$-oxaphosphetanes (**IVb**) have been reported.[19–22] In contrast, the lower coordinate 1,2$\sigma^3\lambda^3$-oxaphosphetanes (**IVa**) were only proposed for a long time, with no known stable derivatives.[23] In 2016, we reported the synthesis of pentacarbonylmetal(0) complexes (M = Cr, Mo, and W) (**V**) either through ring expansion of epoxides using highly reactive Li/Cl phosphinidenoid complexes or ring formation through intramolecular nucleophilic attack in a α,ω-bifunctional phosphane complex.[24–26] Recently, we also gained access to the free ligand[27] (**IVa**) using thermal decomplexation[28] from complexes [M(CO)$_5$L] based on the chelating properties of bis(diphenylphosphino)ethane (DPPE). The first SC-XRD structure of a non-ligated 1,2$\sigma^3\lambda^3$-oxaphosphetane (**IVa**) was reported together with examples of P-oxidation reactions using *ortho*-chloranil and P-complexation by gold(I) chloride.[27] Subsequently, we reported on an elusive 1,2$\sigma^4\lambda^5$-oxaphos-phetane P-oxide (**VI**) and also on a stable P-sulfide and a P-selenide, formerly unknown.[29]

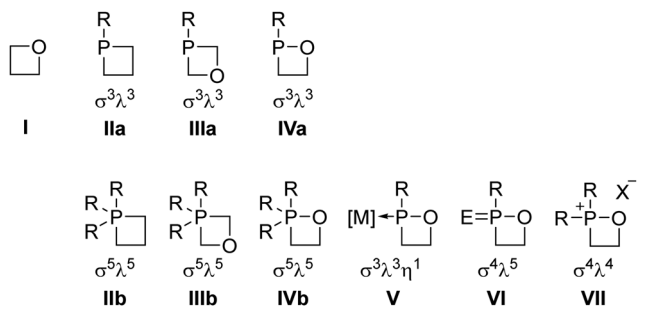

Fig. 1 Oxetane (**I**), phosphetanes ($\sigma^3\lambda^3$ **IIa**, $\sigma^5\lambda^5$ **IIb**), 1,3-oxaphosphetanes ($\sigma^3\lambda^3$ **IIIa**, $\sigma^5\lambda^5$ **IIIb**), 1,2-oxaphosphetanes ($\sigma^3\lambda^3$ **IVa**, $\sigma^5\lambda^5$ **IVb**), 1,2$\sigma^3\lambda^3$-oxaphosphetane metal complexes (**V**), 1,2$\sigma^4\lambda^5$-oxaphosphetanes (**VI**) and 1,2$^\sigma$4λ^4-oxaphos-phetan-2-ium (**VII**).

[a] *Institut für Anorganische Chemie, Rheinische Friedrich-Wilhelms-Universität Bonn, Gerhardt-Domagk-Straße 1, 53121 Bonn, Germany*
E-mail: r.streubel@uni-bonn.de
[b] *Facultad de Química, Campus de Espinardo, Universidad de Murcia, 30100 Murcia, Spain. E-mail: artuesp@um.es*

† Dedicated to Prof. Dr Hansjörg Grützmacher on the occasion of his 65th birthday and in memory of Prof. Dr Edgar Niecke, one of the pioneers of modern chemistry of small P-heterocycles.

‡ Electronic supplementary information (ESI) available: Experimental protocols, NMR and theoretical data. CCDC 2290099–2290104. For ESI and crystallographic data in CIF or other electronic format see DOI: https://doi.org/10.1039/d4cc00254g

We became attracted to test the usability of 1,2σ^{3}λ^3-oxaphosphetanes **IVa** as a building block for functional organophosphorus compounds *via* the Arbuzov reaction. The latter is an important and well-studied reaction for acyclic phosphanes,[30,31] bearing a P-alkoxy substituent, with alkyl halides, thus rendering functional phosphane oxides as final products (Scheme 1).[30,32] Cyclic versions of this reaction have been studied so far only for 1,2-oxaphospholanes, but not for smaller P-heterocyclic rings such as in **IVa**.[33,34]

Herein, we report on the synthesis and reactions of 1,2-oxaphosphetanes with various alkyl halides thus rendering a variety of β-halo phosphane oxides **XII** involving transient 1,2-oxaphosphetan-2-ium species **VII** as indicated by DFT calculations. Furthermore, preliminary results of a cationic oligomerization of a 1,2-oxaphosphetane is presented.

To avoid complications from the use of diastereomeric 1,2σ^{3}λ^3-oxaphosphetanes, we first synthesized C^4-unsubstituted and symmetrically C^4-disubstituted 1,2-oxaphosphetane complexes. Li/Cl phosphinidenoid molybdenum complex **1** reacted with oxirane or 1,1′-dimethyloxirane to yield selectively the corresponding 1,2-oxaphosphetane molybdenum(0) complexes **4** (65% yield) and **5** (77% yield) (Scheme 2). To our surprise, the subsequent treatment of toluene solutions of **4** and **5** with DPPE at 80 °C led to partial decomposition in the case of **5**, whereas selective formation of unligated 1,2-oxaphosphetane **6** (70% yield) was observed for **4**.

The outcome for **5** could be somewhat improved by reducing the reaction time from 4 h to 2 h thus enabling to detect a resonance signal at 161.6 ppm in the ^{31}P-NMR spectrum of the reaction mixture which was assigned to **7** (content estimated 18%, by ^{31}P{^{1}H} NMR integration). Our established protocol enabled us to isolate 1,2-oxaphosphetane **6**, but **7** could only be observed as a mixture in solution (Scheme 2).[27,29] Complexes **4** and **5** as well as the "free" 1,2-oxaphosphetane **6** were structurally confirmed *via* single crystal X-ray diffraction (SC-XRD) studies. Interestingly, the structural features of **4** and **6** (Fig. 2) are very similar, *i.e.*, an almost planar ring system and similar bond lengths (see the ESI‡). But the ^{31}P{^{1}H} NMR chemical shifts vary distinctively for both complexes (219.5 ppm (**4**) and 183.9 ppm (**5**)) and the unligated 1,2-oxaphosphetanes (212.1 ppm (**6**) and 161.6 ppm (**7**)).

To explore the reactivity of **6**, it was treated with various activated alkyl halides **8a–d** to achieve alkylation at phosphorus to give 1,2-oxaphosphetan-2-ium salts **9a–d** as intermediates. As

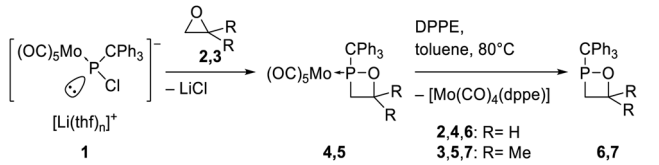

Scheme 2 Synthesis of 1,2-oxaphosphetanes molybdenum complexes **4** and **5** and free 1,2-oxaphosphetanes **6** and **7**.

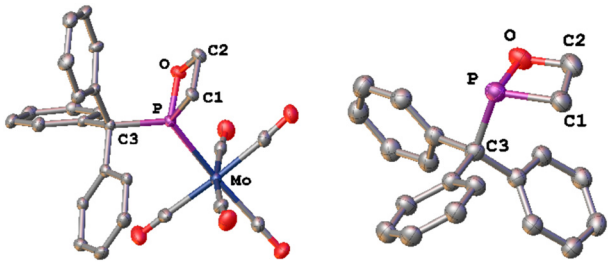

Fig. 2 Molecular structures of **4** (left) and **6** (right) in the solid state. Hydrogen atoms are omitted, and the thermal ellipsoids are set at the 50% probability level. For solid state structures of **5** see the ESI.‡ Selected bond lengths [Å] and angles [°]: **4**: Mo–P 2.487, P–O 1.661(3), P–C1 1.845(5), P–C3 1.895(5), and C1–P–O 80.81(19). **6**: P–O 1.670(3), P–C1 1.849(4), P–C3 1.923(5), and C1–P–O 80.47(18).

acyclic β-halo phosphane oxides **10a–d** were obtained in an Arbuzov-type reaction (Scheme 3), we concluded that a rapid cleavage of the O–C^4 bond upon nucleophilic attack of the counter anion had followed the P-alkylation step instead of forming P-functional 1,2σ^{4}λ^5-oxaphosphetanes. The reactions of **6** with **8a–d** were selective and products **10a–d** were isolated in moderate yields (Table 1). For **10a–c** SC-XRD measurements (Fig. 3) confirmed all proposed structures.

The effect of the counter anion was then examined. While a clean reaction occurred with methyl iodide (**8d**), leading to **10d**, methyl triflate (**8e**) did not enable the reaction of transiently formed **9e** with the counter anion at low temperature, thus behaving as a weakly coordinating anion (WCA).[35,36] Therefore, no "monomeric" molecular compound was formed, and the cationic intermediate **9e** reacted with further units of **6** in propagation steps to give a mixture of oligomeric compounds "**11^n**" (Scheme 4). Analysis of the solid residue of the reaction mixture by MALDI-MS revealed oligomers with up to ten units of **6** incorporated (*m*/*z* 318.1). Repeating the experiment with different equivalents of MeOTf (Fig. 4) showed that, in general, a lesser amount of MeOTf (0.25 eq., 0.05 eq.) led to an increase

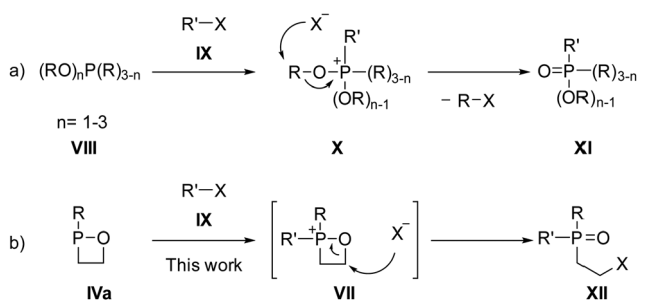

Scheme 1 Examples of Arbuzov reactions for: (a) general, acyclic compounds **VIII**; (b) 1,2σ^{3}λ^3-oxaphosphetanes **IVa**, presented in this work.

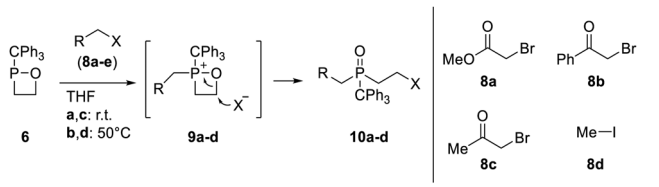

Scheme 3 Arbuzov reactions of **6** yielding β-halo phosphane oxides **10a–d**.

Table 1 $^{31}P\{^{1}H\}$-NMR chemical shift in $CDCl_3$ and yield of **10a–d**

	10a	10b	10c	10d
δ [ppm]	48.4	49.7	48.5	53.6
Yield [%]	42	53	6	57

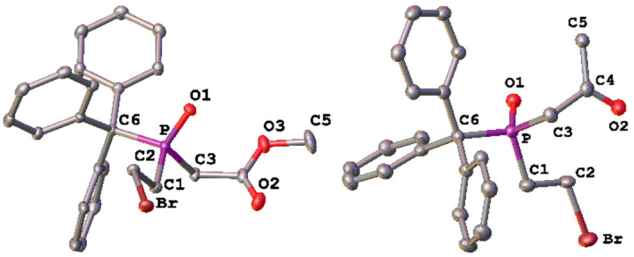

Fig. 3 Molecular structures of **10a** (left) and **10c** (right) in the solid state. Hydrogen atoms are omitted, and the thermal ellipsoids are set at the 50% probability level. For solid state structures of **10b,** see the ESI.‡ Selected bond lengths [Å] and angles [°]: **10a**: P–O 1.4841(10), P–C1 1.8254(14), P–C3 1.8290(14), P–C6 1.8809(14), and C1–P–C3 104.05(7). **10c**: P–O 1.488(3), P–C1 1.823(4), P–C3 1.838(4), P–C6 1.886(3), and C1–P–C3 106.16(17).

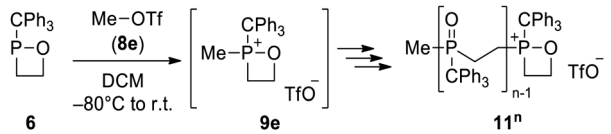

Scheme 4 Arbuzov reaction of **6** with methyl triflate leading to a mixture of oligomers $\mathbf{11}^{n}$ (n = 2–10).

in heavier oligomers **11**,[6–10] but no oligomers with a chain length longer than n = 10 were detected. Dimer $\mathbf{11}^{2}$ formation was favoured for 0.5 eq. of reagent, whereas a pentamer $\mathbf{11}^{5}$ was preferred for all other sub-stoichiometric ratios. The largest relative ratio of heavier oligomers $\mathbf{11}^{6\text{-}10}$ was observed for 0.05 eq. of MeOTf.

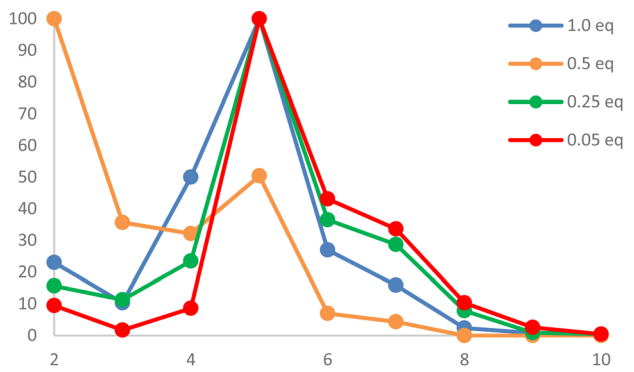

Fig. 4 Relative distribution of chain length of oligomers of $\mathbf{11}^{n}$, depending on equivalents of MeOTf with constant concentration of **6**, as detected by MALDI mass spectrometry.

VT-NMR monitoring showed a complex reaction progress. In the $^{31}P\{^{1}H\}$-NMR spectra, a signal at 130.4 ppm was detected between −80 and −20 °C. This signal is tentatively assigned to the 2-methyl-1,2-oxaphosphetan-2-ium salt **9e**; this was further supported by the calculated ^{31}P chemical shift of 132.5 ppm for the same species (see the ESI‡). Broader signals in the same area were attributed to the propagating 1,2-oxaphosphetan-2-ium end units of growing oligomers $\mathbf{11}^{n}$. A broad signal group from 50 to 58 ppm is assigned to the various open chain phosphane oxide units of the oligomers $\mathbf{11}^{n}$.

While knowing that 1,2-oxaphosphetanes are moderately strained (ring strain energy of the parent compound, RSE = 19.09 kcal mol^{-1} [27]), DFT calculations on the Arbuzov reaction pathway of **6** were performed and, hence, the reaction of the model (*S*)-2-methyl-1,2-oxaphosphetane **6*** with methyl iodide (**8d**) was computed. The primary step is the exergonic P-methylation, affording 2,2-dimethyl-1,2-oxaphosphetan-2-ium iodide **9d*** (Scheme 5 and Fig. 5), which led to a significant increase of the RSE from 18.66 to 26.24 kcal mol^{-1} at the (gas phase) working level of theory,[37] in agreement with the enlarged Lagrangian of the kinetic energy density per electron computed at the ring critical point[38] (G/ρ = 1.1168 and 1.1392 a.u. for **6*** and **9***, respectively), thus paralleling the observed tendency of oxaphosphiranes.[39] The Arbuzov-type reaction of the iodide counter anion in **9d*** is largely facilitated due to the RSE relief, thus proceeding exergonically over a low energy barrier (Fig. 5) and affording β-iodoethyl phosphane oxide **10d***. In the case of using methyl triflate (**8e**) as the methylating agent, the energy barrier is slightly lower (ΔG_{rel} = 23.46 kcal mol^{-1}) and the resulting 1,2-oxaphosphetan-2-ium triflate **9e*** (ΔG_{rel} = –37.35 kcal mol^{-1}) is much more stable than the iodide analogue **9d***. This is due to the presence of a rather strong anion···P bonding interaction with the triflate O^- centre in **9e*** ($d_{P\cdots O}$ = 2.385 Å) than with I^- in **9d*** ($d_{P\cdots I}$ = 3.314 Å). The former highlights the ambiguity of the WCA character of the triflate anion and its inability to promote Arbuzov-type ring opening in **9e***.

Similarly, the reaction of **6** with methyl bromoacetate **8a** occurred selectively giving a β-bromoethyl phosphane oxide, like compound **10a*** in the computed model reaction (Fig. 5 and Scheme 5). Intermediate **9a*** also displays a remarkable pnictogen bonding interaction with the Br^- formal anion ($d_{P\cdots Br}$ = 2.665 Å), but the value is well below the sum of the van-der-Waals radii (1.80 + 1.85 = 3.65 Å). However, α-halocarbonyl compounds feature a second electrophilic site at the carbonyl C atom which can allow for the formation of the Perkow product, in general,[40,41] that was shown to proceed through initial formation of a σ^5 λ^5-oxaphosphirane intermediate.[42] In the case of the reaction of **6*** with methyl bromoacetate (**8d**), the alternative Perkow route

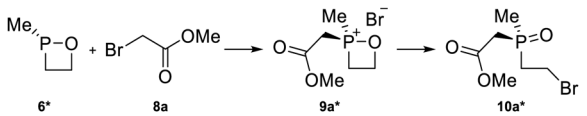

Scheme 5 Reaction of **6*** with methyl bromoacetate **8a**.

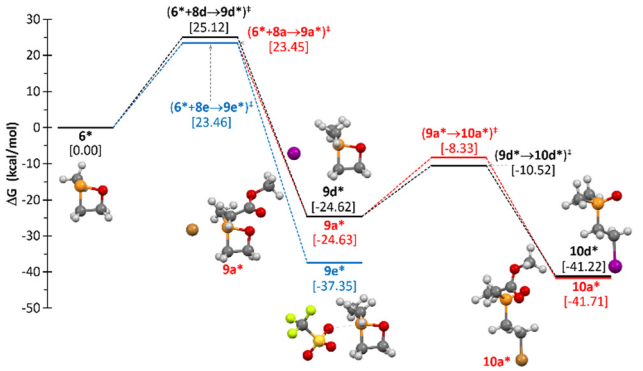

Fig. 5 Computed ($CPCM_{solv}$/PWPB95-D3/def2-QZVPP//$CPCM_{solv}$/PBEh-3c) Gibbs energy profile for the reaction of model **6*** with **8a, d, and e**. Solvent: THF for reaction with **8a and d** but CH_2Cl_2 for **8e**.

was investigated computationally (see the ESI‡) which turned out to be both kinetically and thermodynamically disfavoured compared to the Arbuzov route. The kinetic preference for the Michaelis–Arbuzov pathway can be explained in terms of most favoured frontier molecular orbital (FMO) interactions (*i.e.* the phosphorus lone pair of **6** and the σ*(C–Br)-orbital of **8a**, see the ESI‡). For **8c**, the only observed product is again the thermodynamically most stable Arbuzov product **10c**.

In total, reactions of a C,C-unsubstituted 1,2$\sigma^3\lambda^3$-oxaphosphetane with various organic bromo and iodo derivatives were studied, including methyl triflate, to probe the effect of the counter anion. While bromo and iodo derivatives led cleanly to Arbuzov-type products, the β-halo phosphane oxides, methyl triflate led to a mixture of low-weight oligomers. In the latter case, VT-NMR studies provided evidence for the first 1,2-oxaphosphetan-2-ium salt formed at low temperature, which was also supported by DFT calculations.

FG carried out experiments and evaluated analytical data. GS is responsible for the crystallographic data. RS provided concept and the supervised the investigation. FG, AEF and RS wrote the manuscript. The ESI‡ was prepared by FG, AEF and RS.

We gratefully acknowledge financial support from the Deutsche Forschungsgemeinschaft and the University of Murcia for the computational resources of Servicio de Cálculo Científico (SCC).

Conflicts of interest

There are no conflicts to declare.

Notes and references

1 G. He, O. Shynkaruk, M. W. Lui and E. Rivard, *Chem. Rev.*, 2014, **114**, 7815.
2 J. A. Bull, R. A. Croft, O. A. Davis, R. Doran and K. F. Morgan, *Chem. Rev.*, 2016, **116**, 12150.
3 R. Klein and F. R. Wurm, *Macromol. Rapid Commun.*, 2015, **36**, 1147.
4 A. Marinetti and D. Carmichael, *Chem. Rev.*, 2002, **102**, 201.
5 W. Zhao, P. K. Yan and A. T. Radosevich, *J. Am. Chem. Soc.*, 2015, **137**, 616.
6 K. D. Reichl, N. L. Dunn, N. J. Fastuca and A. T. Radosevich, *J. Am. Chem. Soc.*, 2015, **137**, 5292.
7 T. V. Nykaza, T. S. Harrison, A. Ghosh, R. A. Putnik and A. T. Radosevich, *J. Am. Chem. Soc.*, 2017, **139**, 6839.
8 L. Longwitz, A. Spannenberg and T. Werner, *ACS Catal.*, 2019, **9**, 9237.
9 L. Longwitz and T. Werner, *Pure Appl. Chem.*, 2019, **91**, 95.
10 L. Longwitz and T. Werner, *Angew. Chem., Int. Ed.*, 2020, **59**, 2760.
11 B. Kaboudin, H. Haghighat and T. Yokomatsu, *Synthesis*, 2011, 3185.
12 G. Wittig and G. Geissler, *Justus Liebigs Ann. Chem.*, 1953, **580**, 44.
13 A. Hinz, R. Labbow, C. Rennick, A. Schulz and J. M. Goicoechea, *Angew. Chem., Int. Ed.*, 2017, **56**, 3911.
14 G. Wittig and U. Schöllkopf, *Chem. Ber.*, 1954, **87**, 1318.
15 E. Vedejs, G. P. Meier and K. A. J. Snoble, *J. Am. Chem. Soc.*, 1981, **103**, 2823.
16 G. Wittig and W. Haag, *Chem. Ber.*, 1955, **88**, 1654.
17 A. Espinosa Ferao, *ChemPlusChem*, 2023, e202300474.
18 A. Espinosa Ferao, *Inorg. Chem.*, 2018, **57**, 8058.
19 U. Dieckbreder, E. Lork, G.-V. Röschenthaler and A. A. Kolomeitsev, *Heteroat. Chem.*, 1996, **7**, 281.
20 M. Hamaguchi, Y. Iyama, E. Mochizuki and T. Oshima, *Tetrahedron Lett.*, 2005, **46**, 8949.
21 T. Kawashima, K. Kato and R. Okazaki, *Angew. Chem., Int. Ed. Engl.*, 1993, **32**, 869.
22 Mazhar-ul-Haque, C. N. Caughlan, F. Ramirez, J. F. Pilot and C. P. Smith, *J. Am. Chem. Soc.*, 1971, **93**, 5229.
23 E. N. Dianova, E. Y. Zabotina, I. Z. Akhmethkhaova and Y. D. Samuilov, *Zh. Obshch. Khim.*, 1991, 1063.
24 A. W. Kyri, G. Schnakenburg and R. Streubel, *Chem. Commun.*, 2016, **52**, 8593.
25 A. W. Kyri, *Investigations on 1,2-Oxaphosphetane Complexes*. PhD Thesis, University of Bonn, Germany, 2017.
26 A. W. Kyri, V. Nesterov, G. Schnakenburg and R. Streubel, *Angew. Chem., Int. Ed.*, 2014, **53**, 10809.
27 A. W. Kyri, F. Gleim, A. García Alcaraz, G. Schnakenburg, A. Espinosa Ferao and R. Streubel, *Chem. Commun.*, 2018, **54**, 7123.
28 A. Espinosa Ferao, B. Deschamps and F. Mathey, *Bull. Soc. Chim. Fr.*, 1993, 695.
29 F. Gleim, A. García Alcaraz, G. Schnakenburg, A. Espinosa Ferao and R. Streubel, *Molecules*, 2022, **27**, 3345.
30 B. A. Arbusow, *Pure Appl. Chem.*, 1964, **9**, 307.
31 A. Michaelis and R. Kähne, *Ber. Dtsch. Chem. Ges.*, 1898, **31**, 1048.
32 A. K. Bhattacharya and G. Thyagarajan, *Chem. Rev.*, 1981, **81**, 415.
33 S. Kobayashi, M. Suzuki and T. Saegusa, *Macromolecules*, 1984, **17**, 107.
34 F. Mathey and F. Mercier, *J. Chem. Soc., Chem. Commun.*, 1980, **0**, 191.
35 G. A. Lawrance, *Chem. Rev.*, 1986, **86**, 17.
36 I. Krossing and I. Raabe, *Angew. Chem., Int. Ed.*, 2004, **43**, 2066.
37 RSE 20.19 (6*) and 27.62 kcal mol^{-1} (9*), at the standard DLPNO-CCSD(T)/def2-QZVPP//B3LYP-D4/def2-TZVP level of theory.
38 A. Espinosa Ferao, *Tetrahedron Lett.*, 2016, **57**, 5616.
39 A. Espinosa Ferao, A. Rey Planells and R. Streubel, *Eur. J. Inorg. Chem.*, 2021, 348.
40 W. Perkow, K. Ullerich and F. Meyer, *Sci. Nat.*, 1952, **39**, 353.
41 W. Perkow, *Chem. Ber.*, 1954, **87**, 755.
42 A. Espinosa Ferao, *J. Phys. Chem. A*, 2017, **121**, 6517.

